Geomechanics and Engineering, *Vol. 37, No. 2 (2024) 109-122*
https://doi.org/10.12989/gae.2024.37.2.109

A novel triaxial testing device for unsaturated soils with measurement of suction and volumetric strains

Qian-Feng Gao[1,2a], Mohamad Jrad*[2], Mahdia Hattab[2b], Said Taïbi[3c] and Jean M. Fleureau[4d]

[1]*School of Traffic & Transportation Engineering, Changsha University of Science & Technology, Changsha 410114, China*
[2]*Laboratoire d'Étude des Microstructures et de Mécanique des Matériaux, Université de Lorraine – CNRS UMR 7239, Arts et Métiers ParisTech, Metz, France*
[3]*Laboratoire LOMC, Université Le Havre Normandie & CNRS, Le Havre, France*
[4]*Laboratoire de Mécanique de Paris-Saclay, Université Paris-Saclay, CentraleSupélec, ENS Paris-Saclay, CNRS UMR 9026, 3 Rue Joliot Curie, 91190 Gif-sur-Yvette, France*

(*Received April 13, 2023, Revised October 12, 2023, Accepted January 13, 2024*)

Abstract. Standard triaxial cells are commonly used to measure the mechanical behavior of saturated soils. However, this type of standard system is difficult to use for unsaturated soil specimens since it cannot measure the changes in the pore-air volume and pressure. This paper proposes to extend the measurement possibilities of the standard triaxial testing device in a simple way and to adapt it to partially saturated soils. The system is supplied by two hygrometers installed at each end of the cylindrical unsaturated specimen to measure local relative humidity, which allows the derivation of suction. The volumetric strain of the specimen is calculated by analyzing digital photos captured from the outside of the transparent cell wall. Specimens made of kaolin clay, having different hydraulic properties, were tested to verify the reliability of the measurements, and thus, the relevance of the proposed techniques to study the mechanical behavior of unsaturated soils.

Keywords: hygrometer; suction; triaxial test; unsaturated soil; volume change

1. Introduction

Unsaturated soil mechanics is an essential part of soil science and geotechnical research. Scientists and geotechnical engineers are interested in understanding the behavior of unsaturated soils under mechanical loadings Sivakumar *et al.* (2013) to model various structures such as shallow foundations Garakani *et al.* (2020), road pavements Goual *et al.* (2011), soil slopes Nguyen and Likitlersuang (2019), subway tunnels Fan *et al.* (2020), retaining walls Chehade *et al.* (2020), tailing dams Bella (2021), landfills (Zhou *et al.* 2014) and railway embankments Kumar *et al.* (2022). From a fundamental point of view, experimental investigations and theoretical analyses are needed to take into account the simultaneous presence of three phases in the soils: liquid, gas and solid (Lin *et al.* 2018). Soil suction is generated by the co-existence of the liquid and gas phases within the soil matrix and significantly influences the mechanical behavior of unsaturated soils. Specific testing methods and techniques were therefore proposed to control and measure suction during tests in the laboratory (Delage *et al.* 2008, Fleureau *et al.* 1993). Volume change monitoring is an additional issue to consider during the tests.

*Corresponding author, Ph.D.
E-mail: mohamad.jrad@univ-lorraine.fr
[a]Ph.D.
[b]Professor
[c]Professor
[d]Professor

The shrinkage phenomenon of clays on the drying path causes the development of suction in the material (Garakani *et al.* 2020). This behavior, placed in the unsaturated soil behavior framework, may experimentally be defined through the Soil-Water Characteristic Curves (SWCC), which express the relationship between the volumetric water content and soil suction. Fleureau *et al.* (1993) reported that the SWCC curve can be obtained with different techniques depending on the suction level. They showed for instance that the axis translation or pressure plate technique, which will be detailed below, is more reliable when the suction values are between 10 kPa and 1500 kPa; on the other hand, the filter paper technique, based on a calibration curve between the water content of the filter paper and suction, may be appropriate to measure suctions ranging from 1500 kPa to 300 MPa. For higher suctions they showed that the saturated salt solutions method, based on the vapor equilibrium technique, allowed to reach the range of suctions from 5 MPa to 500 MPa by controlling the relative humidity of a closed system, as confirmed for instance by Wei *et al.* (2021).

For unsaturated soils under mechanical loading, the control and the measurement of unsaturated parameters obviously need to be carried out with great care. Focusing on triaxial loading, two parameters, i.e., the suction evolution and the volumetric strain variation, are especially difficult to manage during loading. The review paper of Delage (2002) may here be mentioned, where the development of unsaturated testing techniques was described in details, including the techniques of direct suction measurements based on high capacity tensiometers and high suction measurements based on high range psychrometers.

Copyright © 2024 Techno-Press, Ltd.

ISSN: 2005-307X (Print), 2092-6219 (Online)

To measure suction in soils, two types of methods are generally used, i.e., direct methods and indirect methods (Pan *et al.* 2010, Sreedeep and singh 2011). The direct methods are based on matric suction measurement using a porous ceramiccup. The estimation of matric suction requires a full separation between the air phase and the water phase with a ceramic disk. The direct measurement devices include tensiometers and suction probes. However, the measurement range with this method is limited to around 1.5 MPa due to cavitation. The indirect method is usually based on the determination of a physical parameter such as relative humidity, electrical or thermal conductivity. Accordingly, the sensors include electrical conductivity sensors, thermal conductivity sensors, psychrometers and chilled mirror hygrometers. Advantages and drawbacks of these methods were discussed and complementarities between them should be considered. Fondjo *et al.* (2020) focused on various methods for soil suction measurements. They carried out a comparative study on direct and indirect suction estimations, detailed measurement ranges, processing time and limitations. They stated that the chilled-mirror hygrometer and the filter-paper technique are cost-effective techniques with a wide range of suction measurements; however, the chilled-mirror hygrometer technique is more precise and does not require as much care as the filter paper technique for which need a large proceeding time of several days is necessary. The long proceeding time needed with the filter paper technique limits its application in triaxial testing. Cardoso *et al.* (2017) presented a small sol-gel humidity sensor incorporated inside soil specimens for measuring suction between 1 MPa and 10 MPa; however, further improvements are needed in terms of calibration protocol.

The suction-controlled triaxial apparatus developed by Bishop and Donald (1961) is a variant from the classical triaxial testing machine. It is an axis translation technique-based device that allows to perform unsaturated triaxial tests on various soils, which is of particular scientific interest. With this type of test, in addition to the mechanical data (radial and axial stresses applied to the specimen, and axial strain), special attention should be given to: i) suction control and measurement; ii) the measurement of specimen volume change, which is a delicate problem. In a geotechnical testing system, three methods are often used to control suction inside a specimen. One of the methods is the axis translation technique, which shifts the pore-water pressure to a positive value and measures or controls the matric suction by increasing the reference pore air pressure inside the specimen. This method was used commonly in the determination of SWCC and adapted to oedometer and triaxial devices (Aversa and Nicotera 2002, Ng *et al.* 2007, Jiang *et al.* 2021). However, this method cannot appropriately reflect the real in-situ conditions since it raises the pore air pressure. The second method is the osmotic technique (Delage and Cui 2008, Derfouf *et al.* 2020). In this method, the specimen is placed on a semi-permeable membrane. Then a solution containing polyethylene glycol is circulated in the specimen, and only water is able to go through the membrane. Depending on the concentration of the solution, different levels of osmotic suction are applied to the specimen. This method was applied to the oedometer and triaxial testing devices, but special attention should be paid to the life duration of the membrane when using this kind of method. Another method is the vapor equilibrium technique, which controls the relative humidity in a sealed volume through a salt solution (Baltz and Graham 2000, Blatz *et al.* 2008, Ferrari *et al.* 2018). Water molecules migrate from the soil pores to the vapor phase before the equilibrium state is reached.

Three types of methods can be mentioned to measure the volume changes of saturated soils: (i) the measurement of the fluid volume change inside the specimen via a high-precision volume change gauge; (ii) the measurement of the volume change of the triaxial cell water (the accuracy is affected by the compression of air in the triaxial cell and the deformation of the cell); and (iii) the direct measurement of specimen deformation via the laser technique, local axial and radial strain sensors, and digital photography (Rifa'i *et al.* 2002, Laloui *et al.* 2006). However, the measurement of volume changes of unsaturated soil specimens during the mechanical loading is more complex because the volume depends on the exchange and compression of air and water, which are both compressible. In this case, one of the feasible methods is to use the HKUST inner cell volume measurement device Ng *et al.* (2002), which is based on the variations in the differential pressure because of the changes in the water level in an inner cell. The recorded values are used to obtain the total volume change in an unsaturated soil specimen. Another method is the double cell or double wall volume measurement Estabragh and Javadi (2012), which avoids the error caused by the cell wall deformation in classical triaxial cells. The volume change of a specimen is determined by the volume change in the inner cell. The third method is to use local sensors fixed directly on the test specimen (Laloui *et al.* 2006). Local sensors allow to separately measure the axial strain and the radial strain, and thus the volumetric strain can be calculated. The fourth method is the digital photographic method (Fan *et al.* 2020). Concerning the image analysis method, the drawbacks are due to light refraction problems. Hence, this method need to be calibrated before being applied to measure the volumetric strain of the specimen deformation. Despite these limitations, this method is most promising because it relies only on a CCD camera (no intricate devices are required) and has no interference with the specimen. (Chehade *et al.* 2020).

Most of the above techniques are very complex and difficult to apply in practice. This paper aims to provide simplified tests for unsaturated triaxial loading. Several techniques (presented in the introduction section) exist, requiring specific and complex experimental setup. The two key points specific to the unsaturated tests are: i- the suction control and measurement; ii- the volume strain monitoring. Most of the suction measurement methods of the literature have a limited range, or need long of time to acquire measurement. This paper proposes an original method based on new self-sufficient and tiny hygro-button sensor.

The latter consists in controlling the initial suction of specimens using the traditional salt solutions method, supported by a tiny hygro-button sensor to measure suction

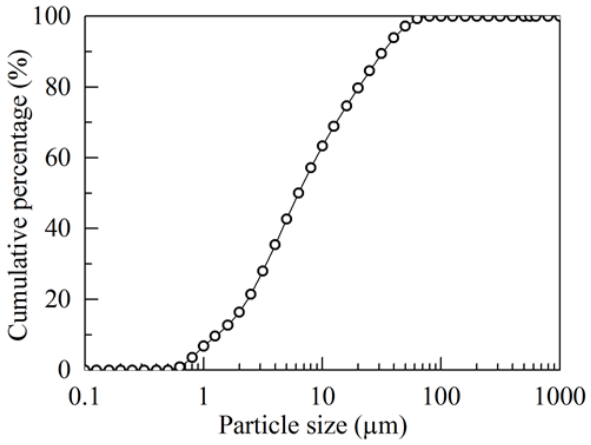

Fig. 1 Particle size distribution of kaolin clay

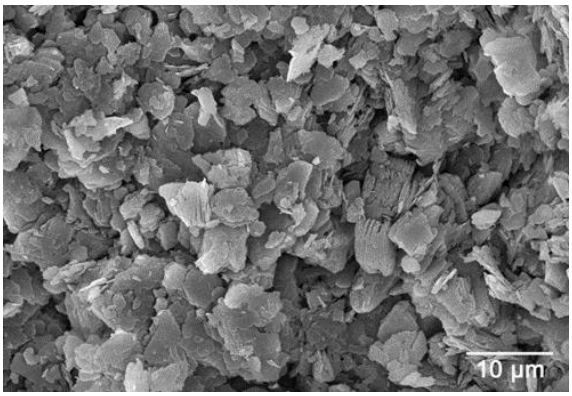

Fig. 2 SEM image of kaolin clay

variations during triaxial tests. Image analysis was chosen for the volume strain monitoring.

2. Materials and preparation of partially saturated specimens

The studied material is a pure kaolin clay (kaolin K13) supplied by the Sibelco company. The specific gravity of the solid matrix is 2.63. The plastic limit and liquid limit are w_P = 20% and w_L = 42%, respectively. The specific surface area of the material, as determined by the methylene blue method, is approximately 27 m^2/g.

Fig. 1 presents the "particle size distribution" of the original material obtained by the laser grain size analysis. The "particle size" here may represent the "aggregate size" in reality. It is noted that about 60% of the soil aggregates are smaller than 9 μm, which is in agreement with the information obtained from scanning electron microscopy (SEM) observations (Fig. 2). The geotechnical parameters of this clay are reported in previous studies such as (Gao *et al.* 2020, Zhao *et al.* 2019).

The triaxial test specimens were prepared from a clay slurry, following the procedures used for instance by Zhao *et al.* (2019). The clay slurry had an initial water content of 1.5 w_L (w_L is the liquid limit) and was preconsolidated in a consolidometer under a vertical effective stress of 120 kPa. Afterward, cylindrical specimens (height = 75 mm and

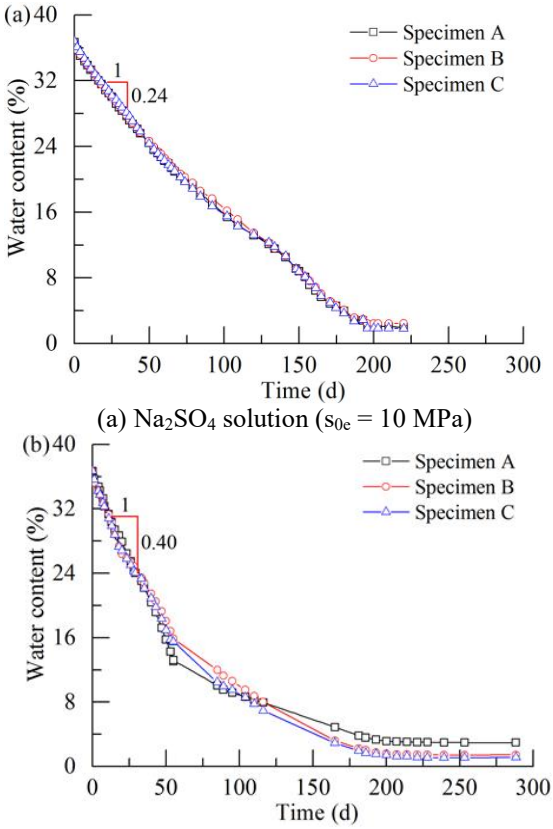

(a) Na_2SO_4 solution (s_{0e} = 10 MPa)

(b) NaCl solution (s_{0e} = 38 MPa)

Fig. 3 Water content evolution of remolded kaolin clay specimens in desiccators

Table 1 Saturated salt solutions for suction control

Salt solution	Temperature T (℃)	Relative humidity RH (%)	Total suction s_{0e} (MPa)
NaCl	20	76	38
Na_2SO_4	20	93	10
$CaSO_4$	20	98	3

diameter = 50 mm) were extracted from the preconsolidated clay core. As several authors recommended (Bishop and Green 1965, Biarez 1962, Hattab and Hicher 2004) weak height to diameter ratio (about 1.5 to 1) were used combined with anti-friction system. The latter set up allows to significantly reduce the strain and stress heterogeneities while reducing the friction effects at the ends of the sample. The vapor equilibrium method was then employed to impose suction on unsaturated clay specimens. This was realized by placing the clay specimens in the atmosphere of saturated salt solutions in desiccators. Since too high suctions may cause cracks in the specimens and too small suctions may cause notable measurement errors, as will be discussed later, moderate suction levels between 3 MPa and 38MPa were chosen. The saturated salt solutions used in the current research are listed in Table 1. The relative humidity (RH) and temperature in the testing room were kept approximately constant (i.e., RH = 50±2% and Temperature = 20±1°C).

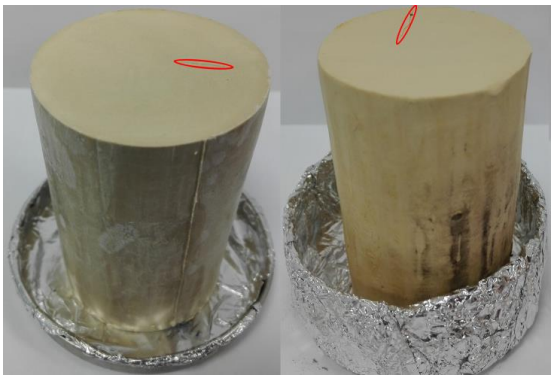

Fig. 4 Open cracks on the surface of cylindrical specimens of kaolin clay (s_{0e} = 38 MPa)

Fig. 3 shows the change in the gravimetric water contents of the specimens in the desiccator. It is observed that the water content first decreases linearly, then decreases in a nonlinear way, and finally reaches a stabilized value during the whole drying period.

The time for the water content of each specimen to reach equilibrium was generally over 150 days (i.e., 5 months). Moreover, a higher total suction often led to a faster reduction of the water content in the linear phase, and thus a shorter time was needed to reach water content equilibrium. For example, the time to reach equilibrium was about 190 days when the total suction was 10 MPa, and it was shortened to about 150 days when the total suction was 38 MPa. Nevertheless, the reduction of the time to reach equilibrium was not very significant as both levels of total suction (10 MPa and 38 MPa) are very high.

Great caution was taken for specimen preparation during desiccation, especially in the case of the highest total suction of 38 MPa. One sometimes observes open cracks that initiate on the upper surface of the specimens in the linear phase of water content variations. These cracks are associated with the non-uniform shrinkage of the specimen when the drying rate (i.e., the rate of water content reduction) is high. As shown in Fig. 3, the drying rate in the linear phase at a total suction of 38 MPa is considerably larger than the value at a total suction of 10 MPa. Local cracks in Fig. 4 indicate that desiccation cracks might have formed inside the cylindrical kaolin specimens under the highest total suction (38 MPa), which obviously is an issue in the results interpretation and the mechanical behavior analyses. If local and internal cracks develop inside the specimens, they are more difficult to observe and represent a risk of affecting the results. In this study, the specimens containing cracks were systematically excluded with the aid of X-ray radiography to eliminate the above risk.

3. Triaxial testing device for unsaturated soils

Triaxial tests were carried out on cylindrical specimens under unconsolidated undrained (UU) triaxial compression and a given initial suction conditions, using GDS triaxial testing system. The unsaturated triaxial testing setup allow to control and to measure the axial stress, the axial strain,

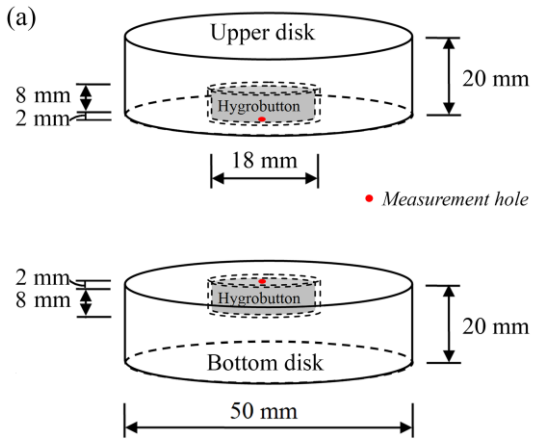

(a) Hygro-buttons in PMMA disks

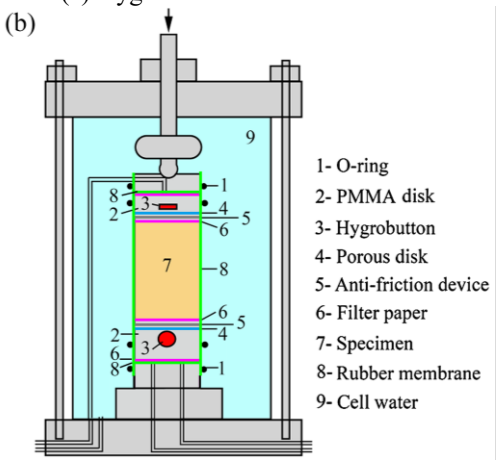

(b) Triaxial testing setup

Fig. 5 Triaxial testing setup with suction measurement

and the confining pressure. The main difficulty of this type of setup consists in the measurement of volume change (hence the volumetric strain) and suction of the unsaturated specimen. In this paper, we propose to use hygro-buttons to measure suction evolution, and digital photography to capture the volume variation during the test.

These two devices as well as the measurement techniques are explained in detail in section 4. Fig. 5 presents the specimen set up in the triaxial cell. All necessary elements such as the anti-friction devices, the filter papers, the rubber membrane, the porous disks, the two hygro-buttons and the polymethyl methacrylate (PMMA) disks used for the total suction measurements inside the triaxial cell, were placed in the same desiccator as the specimen. In this way, the elements were able to reach equilibrium with the specimen. Thus, the installation of these elements would not affect the measurement precision of suction in the specimen during the test. The two hygro-buttons were fixed in the pre-drilled holes of the two PMMA disks, and then they were installed on the bottom and top ends of the soil specimen as shown in Fig. 5. Hence, the evolution of total suction in the vicinity of the specimen ends could be measured indirectly.

The procedure of triaxial tests was divided into two steps. First, the chosen isotropic stress p was applied to the

Table 2 Specification of triaxial tests on kaolin clay

Test type	Number	Specimen	Salt solution	s_{0e} (MPa)	s_0 (MPa)	p (kPa)	p' (kPa)	s_{0i} (MPa)
Saturated triaxial test	1	S0_P200	/	0.0	/	200	200	/
	2	S0_P600	/	0.0	/	600	600	/
	3	S0_P1000	/	0.0	/	1000	1000	/
Unsaturated triaxial test	1	S10_P200	Na_2SO_4	10.0	13.6	200	/	8.3
	2	S10_P600	Na_2SO_4	10.0	10.4	600	/	9.3
	3	S10_P1000	Na_2SO_4	10.0	11.0	1000	/	7.5
	4	S38_P200	NaCl	38.0	40.0	200	/	36.2
	5	S38_P600	NaCl	38.0	37.2	600	/	35.8
	6	S38_P1000	NaCl	38.0	36.9	1000	/	33.1

Note: S_{0e} is the target suction; s_0 is the average measured initial suction; s_{0i} is the average measured suction after isotropic compression; p is the isotropic stress; p' is the effective isotropic stress

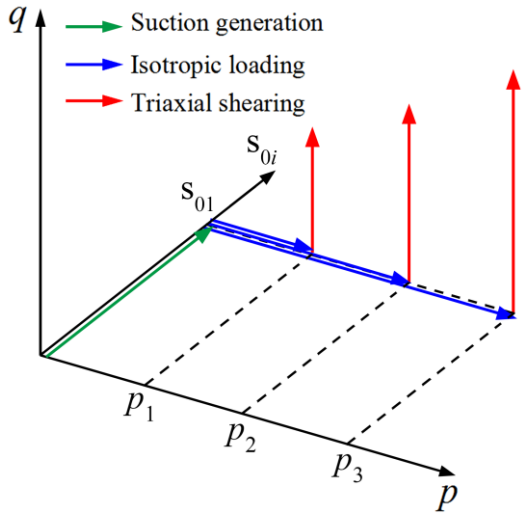

Fig. 6 Stress paths used for unsaturated triaxial testing

specimen in several steps under undrained conditions (both water and air were not discharged). Secondly, triaxial shearing was conducted until the failure of the specimen, as illustrated in Fig. 6. Constant confining pressure was widely used during the shearing step in the literature. However, in order to focus on the effect of deviator stress on the progressive damage of the unsaturated specimen, purely deviatoric stress path, as shown in Hattab and Hicher (2004), was employed in this work.

Unsaturated soils need the equilibrium of negative pore water pressures (or suctions) which requires sufficient time, because of the discontinuity of the liquid phase of the pore water. A low loading rate is necessary in this case to ensure this balance.

In this work, a very small loading rate of 0.007 %/min was employed as recommended by several authors (Mendes and Toll 2016, Hossain and Yin 2010). Under these conditions, the hygro-button can be used to measure the relative humidity.

Table 2 summarizes the soil specimens used in the triaxial tests. Consolidated drained triaxial tests were performed on saturated specimens following the same stress path. During Saturated drained triaxial test null suction condition is maintained representing reference for the different unsaturated tests. On the other hand, for unsaturated undrained tests constant water content was maintained, however suction may vary during the shearing step. Thus, putting together (UU) conditions and saturated CD test allows to study the effect of suction variation on clay behavior. Different initial consolidation was tested in order to study the effect of the mean stress on the suction.

4. Calibration of measurement systems

4.1 Hygro-buttons for suction measurement

The hygro-buttons (Fig. 7) used for suction measurement during triaxial tests are rugged tiny humidity and temperature sensors integrated in a self-sufficient system. Based on a built-in capacitive polymer humidity sensor, a hygro-button is formed of an internal battery, electronic micro-controller, and memory. The recording rate is programmable via computer from 1 s up to 273 h. All the sensor components are assembled in a cylinder of approximately 17 mm in diameter and 6 mm in height. There is a tiny measurement hole on the top of the cylinder, which allows water vapor to pass but repels liquid water. Thanks to its stainless-steel package, it is very durable and highly resistant to environmental hazards (e.g., dust and moisture). At the end of tests, the hygro-buttons are connected to a computer via a special USB reader to import recorded temperature and/or relative humidity. The theoretical measurement range of temperature is from -20°C to +85°C and that of relative humidity is from 0 to 100%. The minimum resolutions are equal to 0.04 % for relative humidity and 0.1°C for temperature. The response time and accuracy of the relative humidity are equal to 30 s and ±5%, respectively. However, capacitive humidity sensors can change their readings when they spend a long time at low (RH< 20%) or high (RH> 80%) relative humidity. This saturation drift effect could be compensated through software using an equation based on laboratory calibration tests. The total suction is expressed as a function of the relative humidity Fredlund and Rahardjo (1993)

Fig. 7 Hygro-button photo and dimensions

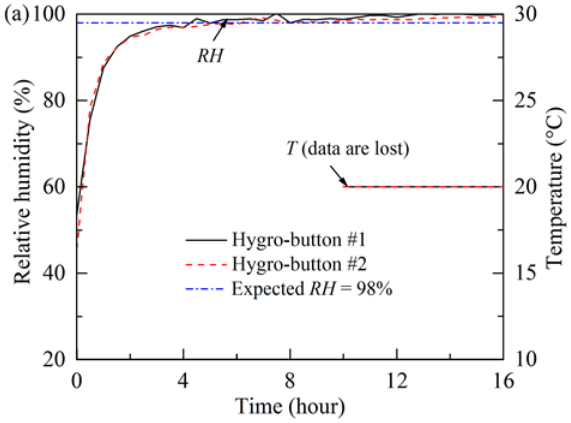

(a) Relative humidity

(b) Global suction

Fig. 8 Calibration of hygro-buttons using $CaSO_4$ solution (s_{0e} = 3 MPa)

$$s = -\frac{R^* T}{v_{w0}\omega_v}\ln(RH) \quad (1)$$

where s is the total suction; R^* is the universal gas constant; T is the absolute temperature; RH is the relative humidity; v_{w0} is the specific volume of water; ω_v is the molecular mass of water vapor. Following these technical characteristics and using Eq. (1), the range of suction measurement is 7-400 MPa.

Before the installation, the hygro-buttons were calibrated via the vapor equilibrium method based on different salts (i.e., $CaSO_4$, Na_2SO_4, and NaCl). Relative humidity and temperature in the laboratory were kept constant at 50% and 20°C, respectively.

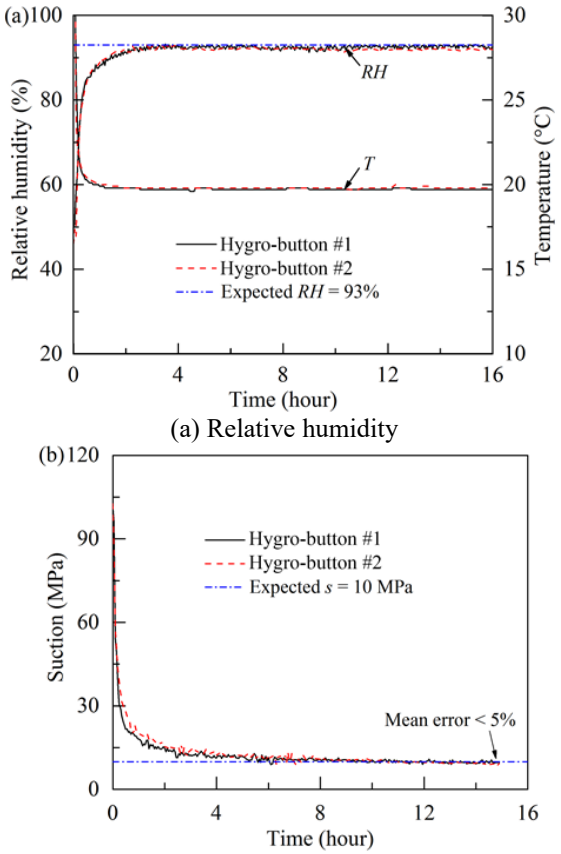

(a) Relative humidity

(b) Global suction

Fig. 9 Calibration of hygro-buttons using Na_2SO_4 solution (s_{0e} = 10 MPa)

The calibration results in Figs. 8-10 show the variation of relative humidity (or total suction) measured by hygro-buttons after they were placed inside desiccators containing the saturated salt solutions. It is noted that the measured relative humidity quickly changes from the laboratory value (50%) to the expected value corresponding to each salt solution. Accordingly, the total suction tends to the expected suction. After 15 h, the measurement error of total suction is less than 5% in the environment of Na2SO4 and NaCl.

However, the relative error between the expected suction obtained with saturated $CaSO_4$ solution and the calculated suction from the measured relative humidity can be larger than 10% (Fig. 8(b)). As the expected relative humidity value was verified with a precise hygro-meter, this means that hygro-buttons are not adapted for relative humidity larger than 95% and, for that reason, this salt was not used in the tests.

Figs. 11 and 12 present the measured relative humidity and total suction of clay specimens during the transition from the desiccator to the triaxial cell. In phase I, the hygro-buttons were transferred from the outside into the desiccator to check if the relative humidity and total suction of the specimen reached the expected values. In phase II, the hygro-buttons, together with the specimen, were transferred from the desiccator into the triaxial cell. Phase III represents the phase after the specimen installation in the triaxial cell. It is noted that the initial relative humidity and total suction approximately meet their target values in the desiccator.

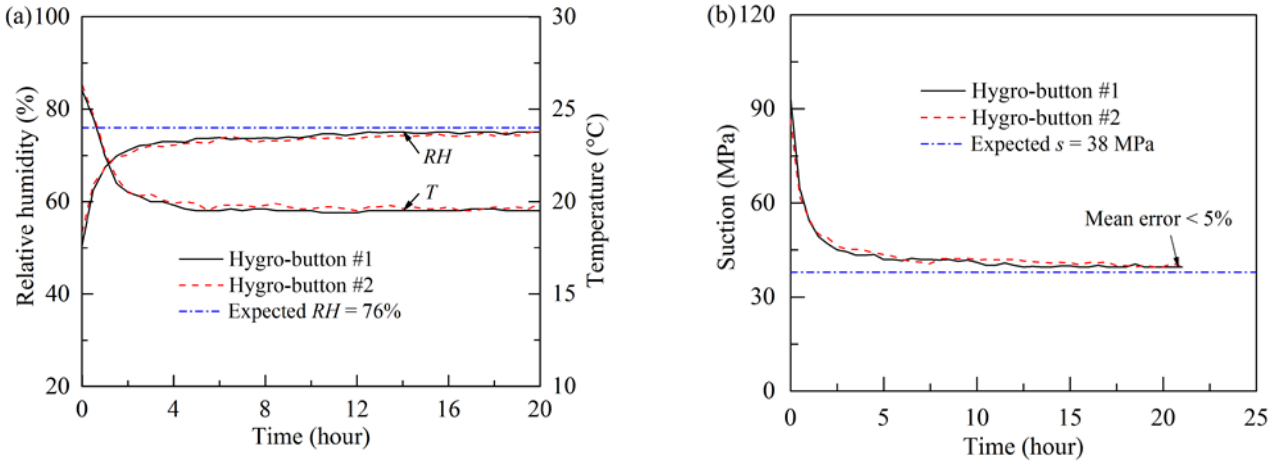

(a) Relative humidity (b) Global suction

Fig. 10 Calibration of hygro-buttons using NaCl solution (s_{0e} = 38 MPa)

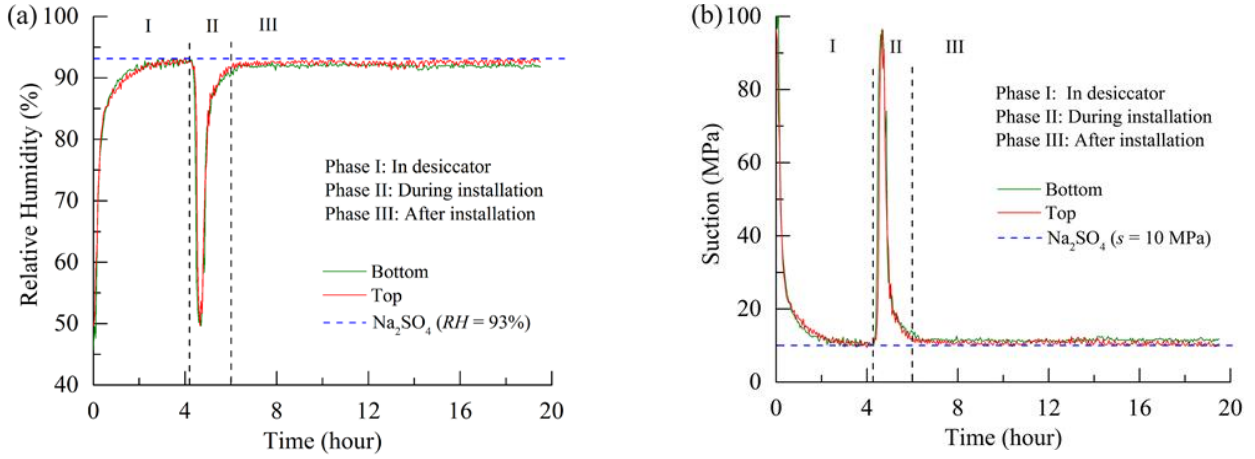

(a) Relative humidity (b) Global suction

Fig. 11 Measured data before triaxial tests (Na_2SO_4, s_{0e} = 10 MPa)

During the specimen installation process, the relative humidity shows an obvious drop due to the disturbance of the laboratory environment; meanwhile, the total suction exhibits a marked rise accordingly.

However, the values of both relative humidity and total suction come back to their initial values a few hours after the sealing of the specimen by the rubber membrane in the triaxial cell. Therefore, it is concluded that the target total suction is successfully reached in the cylindrical specimens. These observations validate the proposed configuration of hygro-buttons and the setup inside the triaxial cell.

4.2 Calibration of strains measurements

During triaxial tests, photos of the specimen were recorded regularly, and the post-analysis of the obtained photos allowed to calculate the volume change as recommended for instance by (Rifa'i *et al.* 2002, Laloui *et al.* 2006). The method consists in capturing photos of the specimen through the transparent triaxial cell with a digital camera during the test. Lamps were placed on two sides of the triaxial cell to provide uniform lighting. The camera was installed in front of the triaxial cell, and its lens was at the same height as the center of the specimen. After triaxial testing, the image analysis method was used to analyze the axial and radial strains of the specimen.

The image processing (Fig. 13) starts with image contrast enhancement, followed by a threshold adjustment to obtain binary image of the specimen. After cleaning and filling back holes, discrete profile curves in pixels are obtained by counting the number of white pixels on both sides of the axis of symmetry of the specimen (Gachet *et al.* 2007). Six measurements along the specimen height and width are used to calculate the axial and the radial strains by the following formulas

$$\varepsilon_r = \left(\sum_{i=1}^{6} \frac{b_i - b_{i0}}{b_{i0}}\right) / 6 \tag{2}$$

$$\varepsilon_1 = \left(\sum_{j=1}^{6} \frac{h_j - h_{j0}}{h_{j0}}\right) / 6 \tag{3}$$

where b_{i0} and b_i are the initial and the current length of the ith horizontal line, respectively; h_{j0} and h_j are the initial length and the current length of the jth vertical line, respectively.

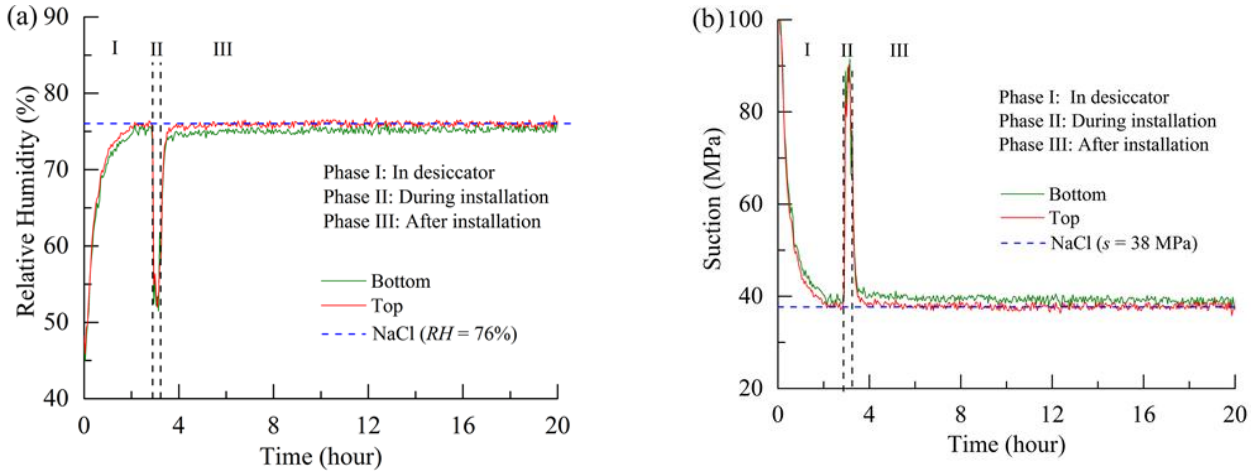

(a) Relative humidity (b) Global suction

Fig. 12 Measured data before triaxial tests (NaCl, s_{0e} = 38 MPa)

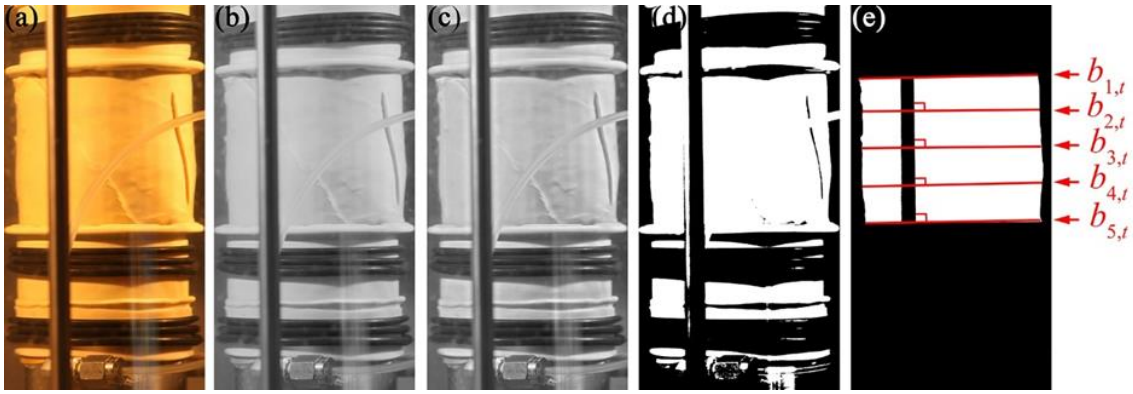

Fig. 13 Image processing steps: (a) original image, (b) greyscale image, (c) image enhancement, (d) thresholding and (e) radial measurements

Eventually, the volumetric strain was derived from the radial and axial strains measured by digital photography. It is important to mention that this method allows to measure the specimen volume change, though potential errors may come from the distortion effects due to the lens curvature, the specimen shape and the light refraction in the triaxial cell wall and the water (Gachet *et al.* 2207, Bhandari *et al.* 2012, Shao *et al.* 2020). In addition, the direction of photography may affect the results as the specimen becomes non-axisymmetric when a shear plane occurs.

To validate the obtained results, an additional triaxial test was conducted on a saturated clay specimen. The measured results of the volumetric strains based on image processing were compared with the usual volumetric strains measured by the pressure-volume controller of the GDS system.

The volumetric strain is calculated by $\varepsilon_v = \varepsilon_1 + 2\varepsilon_r$ on one hand, and derived from the pore water volume change measured by the pressure-volume controller on the other hand. Fig. 14 compares the results from the two methods. It shows that the curves derived from both methods feature a very similar tendency, especially in the first stage of loading. The error on the calculated volumetric strain based on image processing accumulates as the loading goes on due to the distortion effects. However, the maximum error is only about 13% even if the volumetric strain reaches as much as 14%, which indicates that the measurement method using the photos analyses to determine volumetric strains is promising.

To further verify the applicability of the above method to unsaturated triaxial tests, the axial strains of an unsaturated clay specimen (S10_P600) derived from photo analysis during triaxial shearing were compared in Fig. 15 to the axial strain measured by the sensor integrated in the triaxial testing system. It is observed that both calculated and measured axial strains monotonically increase as triaxial shearing begins, showing the same tendency. Moreover, the difference between the calculated and measured axial strain is generally between 0.5% and 1%, which is quite acceptable. This suggests that the indirect method for axial strain determination based on image processing is reliable. Thus, this method to determine the volumetric strain of unsaturated specimens appears to be feasible.

5. Results of unsaturated behavior of kaolin clay

5.1 Suction evolution during triaxial tests

Figs. 16-18 illustrate the evolution of total suctions near

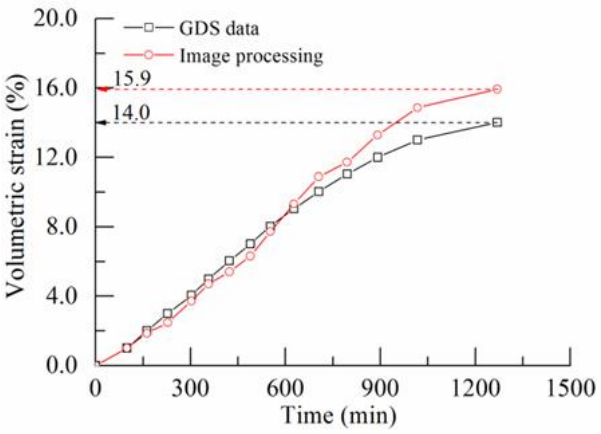

(b) Global suction

Fig. 14 Calibration of volumetric strain measurement during isotropic consolidation of a saturated specimen

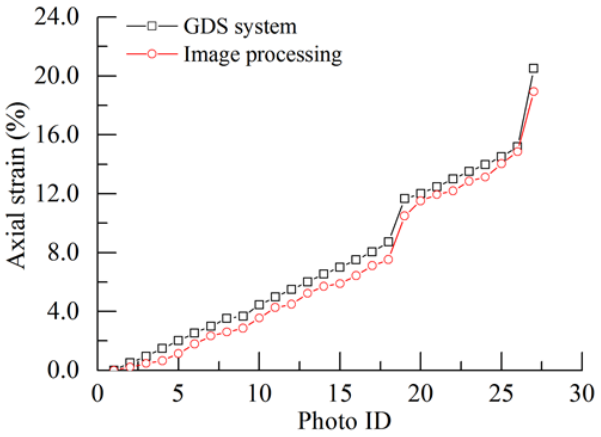

(b) Global suction

Fig. 15 Calibration of strain measurements with specimen S10_P600 as example

the specimen ends measured by the two hygro-buttons. One can note that the suction values of the specimens approach the targets (i.e., 10 MPa and 38 MPa) at the beginning of triaxial testing except for specimen S10_P200, whose initial total suction is slightly higher than the target suction s_{0e} = 10 MPa. During the triaxial tests, the measured total suctions continuously decrease during both compression and shearing stages. It is reasonable because the voids are gradually compressed while water drainage is not allowed, which leads to a rise in the degree of saturation of the soil.

5.2 Evolution of the deviator stress and volumetric strain

Fig. 19 presents the influence of the initial total suction on the stress-strain relationship of the specimen. When the specimen is saturated (i.e., s_{0e} = 0 MPa), in agreement with normally consolidated clay behavior, the deviator stress continuously increases up to a plateau (exhibiting the critical state) with increasing axial strain. By contrast, in the unsaturated state (under the initial suction of s_{0e} = 10 MPa or 38 MPa), the deviator stress first quickly goes up until reaching the peak, then reduces to the residual value as the axial strain increases, characterizing a quasi-brittle failure. It is also noted that the peak deviator stress of the unsaturated specimen is greatly higher than that of the saturated specimen. However, both the peak and residual deviator stresses of the specimen under the global suction of 38 MPa (e.g., S38_P200) are lower than those of the specimen under the lowest global suction of 10 MPa (e.g., S10_P200). The decrease in deviator stress seems to be due to the presence of initial local cracks in the specimen caused by the high suction imposed in the desiccators (Fig. 4).

It should be noted that the gap between the maximum deviator stress of saturated soil and the residual deviator stress of unsaturated soil decreases as the mean stress increases. For instance, when the mean stress is 200 kPa, the maximum deviator stress of the saturated specimen S0_P200 is 171 kPa, and the residual deviator stress of the unsaturated specimen S38_P200 is 267 kPa. However, as the mean stress increases up to 1000 kPa, the maximum deviator stress of the saturated specimen S0_P1000 is 866 kPa, and the residual deviator stress of the unsaturated specimen S38_P1000 is 931 kPa.

Meanwhile, the gap between the maximum deviator stresses of the unsaturated soil at different initial total suctions presents a reducing trend as the mean stress increases. For example, the gap between the maximum deviator stresses of unsaturated specimens S10_P200 and S38_P200 is 57.7% when the mean stress is 200 kPa, whereas the gap between the unsaturated specimens S10_P1000 and S38_P1000 is reduced to 5.0% when the mean stress is 1000 kPa. These findings indicate that the effect of total suction on the unsaturated shear strength of clay is reduced when the mean stress increases.

Additionally, the ratio of deviator stress drops after the peak (i.e., the ratio of the difference between the peak and residual deviator stresses to the peak deviator stress) decreases with an increase in the mean stress. When the initial total suction is 10 MPa, the ratio of deviator stress drop is 37.8% at a mean stress of 200 kPa; by contrast, the ratio decreases to 24.9% at a mean stress of 1000 kPa. The above results suggest that the unsaturated remolded clay becomes less brittle at a higher mean stress. Unsaturated soil is subject to suction which generates internal capillary stresses that tend to over-consolidate the material. In this case, an unsaturated soil subjected to a low mean stress shows an overconsolidated behavior, and thus fragile (or brittle). When the mean stress increases, it tends to erase the overconsolidation due to the suction, and the behavior of the unsaturated soil approaches that of a normally consolidated soil, and thus more ductile (Fleureau *et al.* 1993).

Fig. 20 shows the effect of the initial total suction on the variation of volumetric strains of remolded clay specimens during triaxial shearing. Note that, for unsaturated clays under high suctions, the volumetric strains result from air compression, crack development and shear band formation.

The volumetric strains of saturated clay specimens during triaxial tests performed under drained conditions are always positive, showing contractive behavior (contraction strains are plotted as positive). Nevertheless, the volumetric strains of the unsaturated specimens are first positive

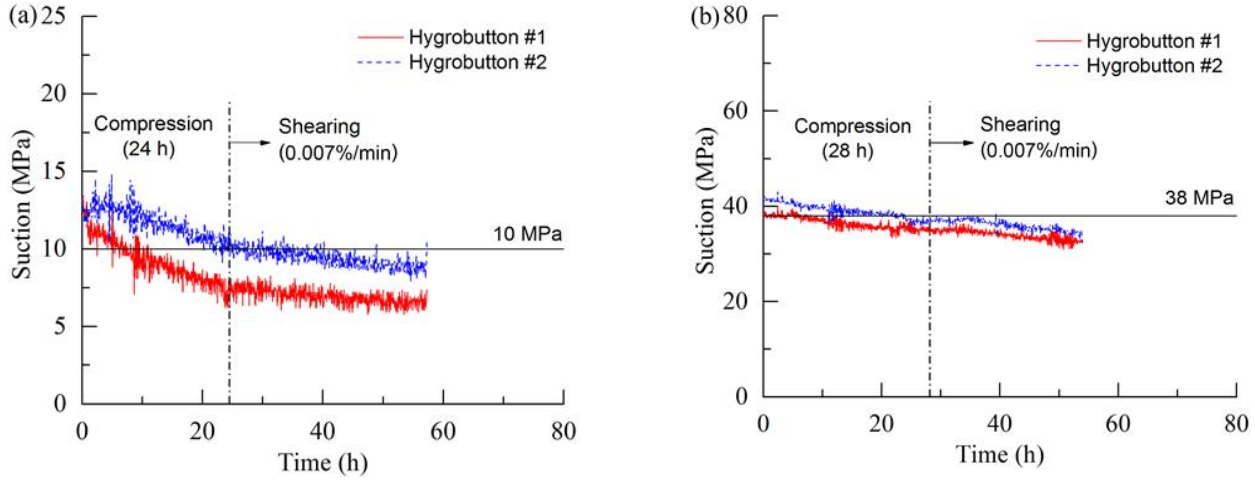

(a) Specimen S10_P200 (b) Specimen S38_P200

Fig. 16 Suction evolution in kaolin clay at a mean stress *p* of 200 kPa during triaxial tests

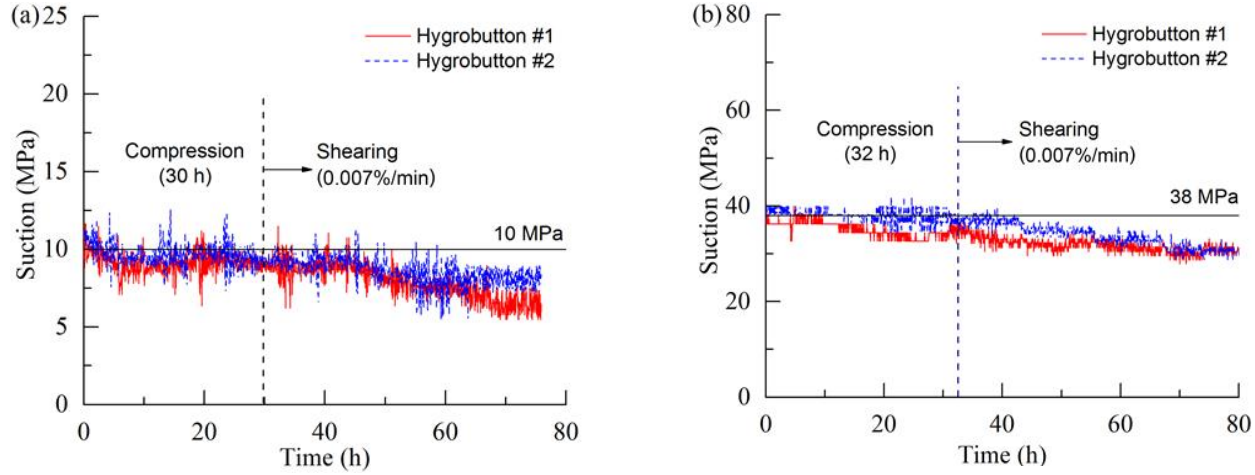

(a) Specimen S10_P600 (b) Specimen S38_P600

Fig. 17 Suction evolution in kaolin clay at a mean stress *p* of 600 kPa during triaxial tests

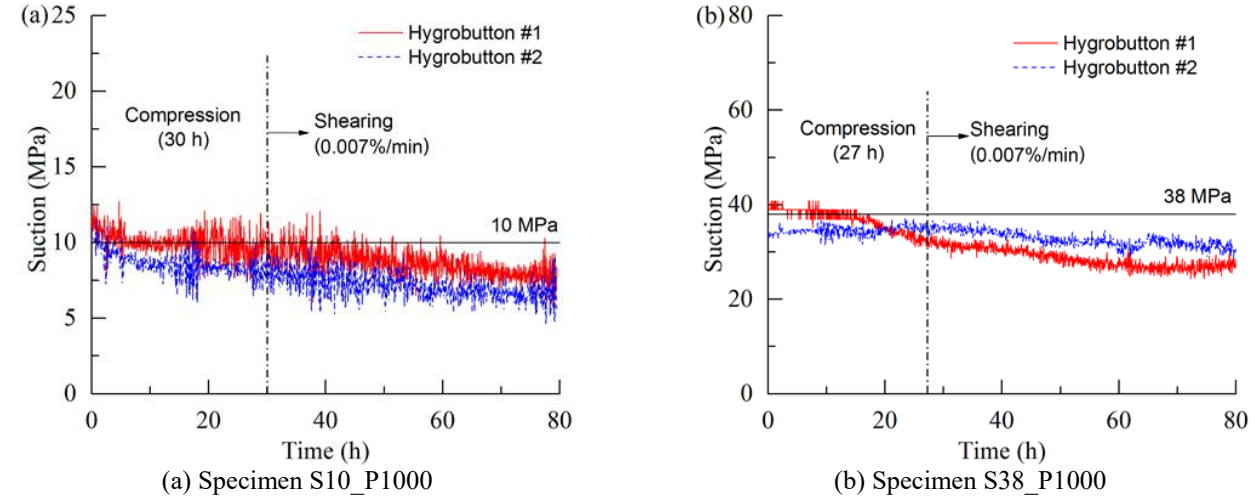

(a) Specimen S10_P1000 (b) Specimen S38_P1000

Fig. 18 Suction evolution in kaolin clay at a mean stress *p* of 1000 kPa during triaxial tests

showing contractive behavior and then negative, i.e., corresponding to dilative behavior, as the axial strains increase.

This first stage seems to be associated with the compression of pore air and the subsequent dilation is dependent on the formation of cracks and shear bands that

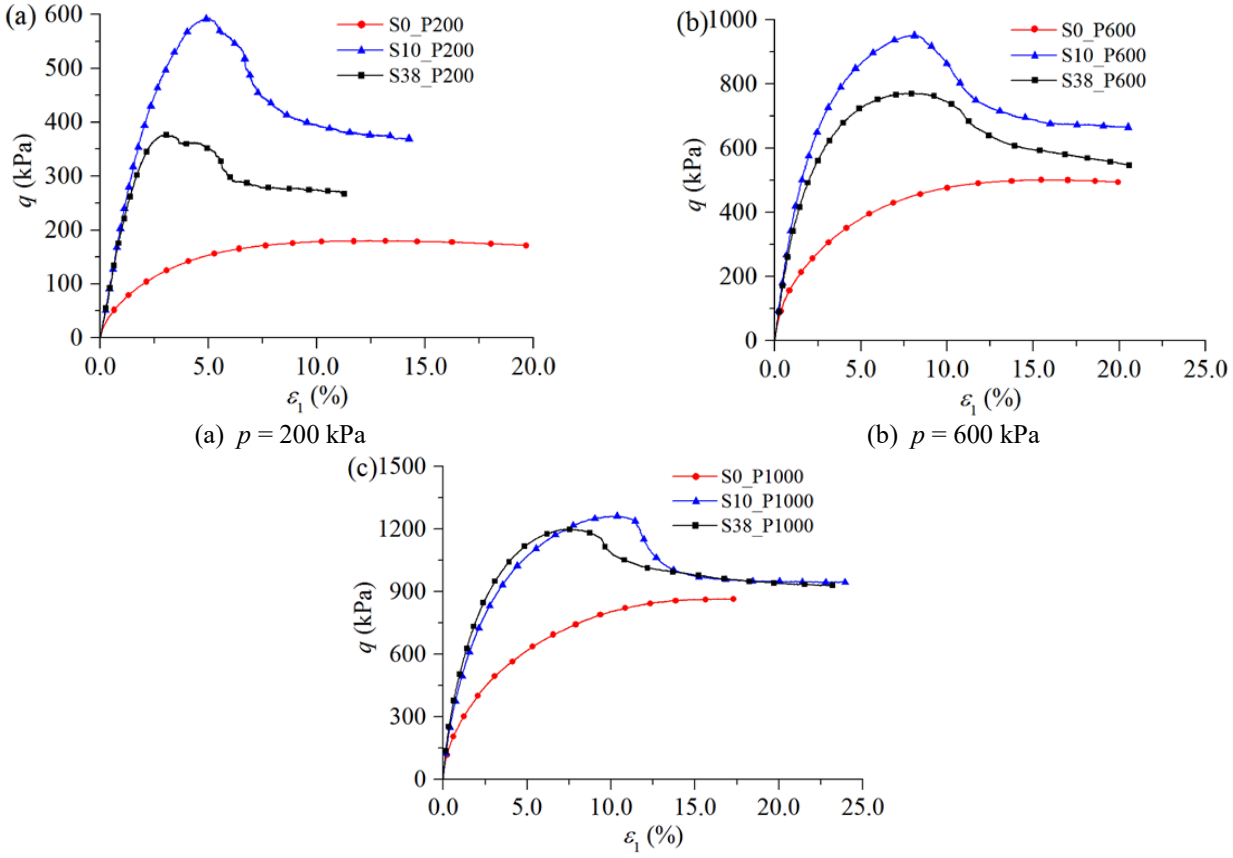

(a) p = 200 kPa (b) p = 600 kPa

(c) p = 1000 kPa

Fig. 19 Stress-strain relationship of kaolin clay at the initial suctions of 0 MPa, 10 MPa and 38 MPa

appear with very slight magnitude in some cases of high suction, or may be attributed to overconsolidation induced by the imposed suction. However, differences are also observed between the different unsaturated clay specimens. For instance, the specimens (e.g., S38_P200 and S38_P600) with a higher initial total suction tend to compress less at the beginning and dilate more at the end. In the case of the specimen S10_P1000 at an initial total suction of 10 MPa, dilation begins at the beginning of the test. The unexpected volumetric strain of this specimen is likely due to the inaccuracy of the 2D photographic technique, as discussed in Section 4.2. Finally, the results indicate that the volumetric behavior of remolded clay is obviously affected by the global suction during triaxial loading.

5.3 Unsaturated behavior described in the (q - ε_v - s) plane

Fig. 21 plots the evolution of total suction in clay specimens during triaxial shearing, for the specimens isotopically consolidated at p = 600 kPa, taken as examples. It must be noted that the total suctions in the first stages of loading are more or less constant. Then, suction tends to decrease slightly before the maximum deviator stress reaches a peak, associated with a strain-softening phenomenon exhibited in Fig. 21(b).

Fig. 22 shows a 3D representation of how the three parameters (suction, volumetric strains and deviator stresses) vary along purely deviatoric stress paths. The three consolidation stresses (p = 200 kPa, 600 kPa and 1000 kPa) are plotted in Fig. 22 for the different initial suctions.

The suctions measured after isotropic loading are indicated by s_{0i} in Table 2. Before shearing, all the curves start from the curve derived from van Genuchten law (Fig. 23) that represents the SWCC curve of the kaolin K13 clay (Cheng *et al.* 2021). The results show that the volumetric strains of the saturated specimens with s_{0e} = 0 MPa increase monotonically, exhibiting contractive behavior well consistent with the normally consolidated behavior of clays. However, the unsaturated specimens, initially submitted to suctions (initially s_{0i}, Table 2) show slight contraction (even no contraction in some cases) in the first stages of the loading followed by a marked dilative behavior. This phenomenon shows the effect of the capillary cohesion induced by the initial suction, the process being accompanied by a decrease of both deviator stress and suction.

6. Conclusions

This study proposed a novel unsaturated triaxial testing system that extends the traditional triaxial cells to measure the mechanical behavior of unsaturated soils. There are two major difficulties regarding this system: (i) traditional triaxial cells cannot control and measure soil suction; (ii)

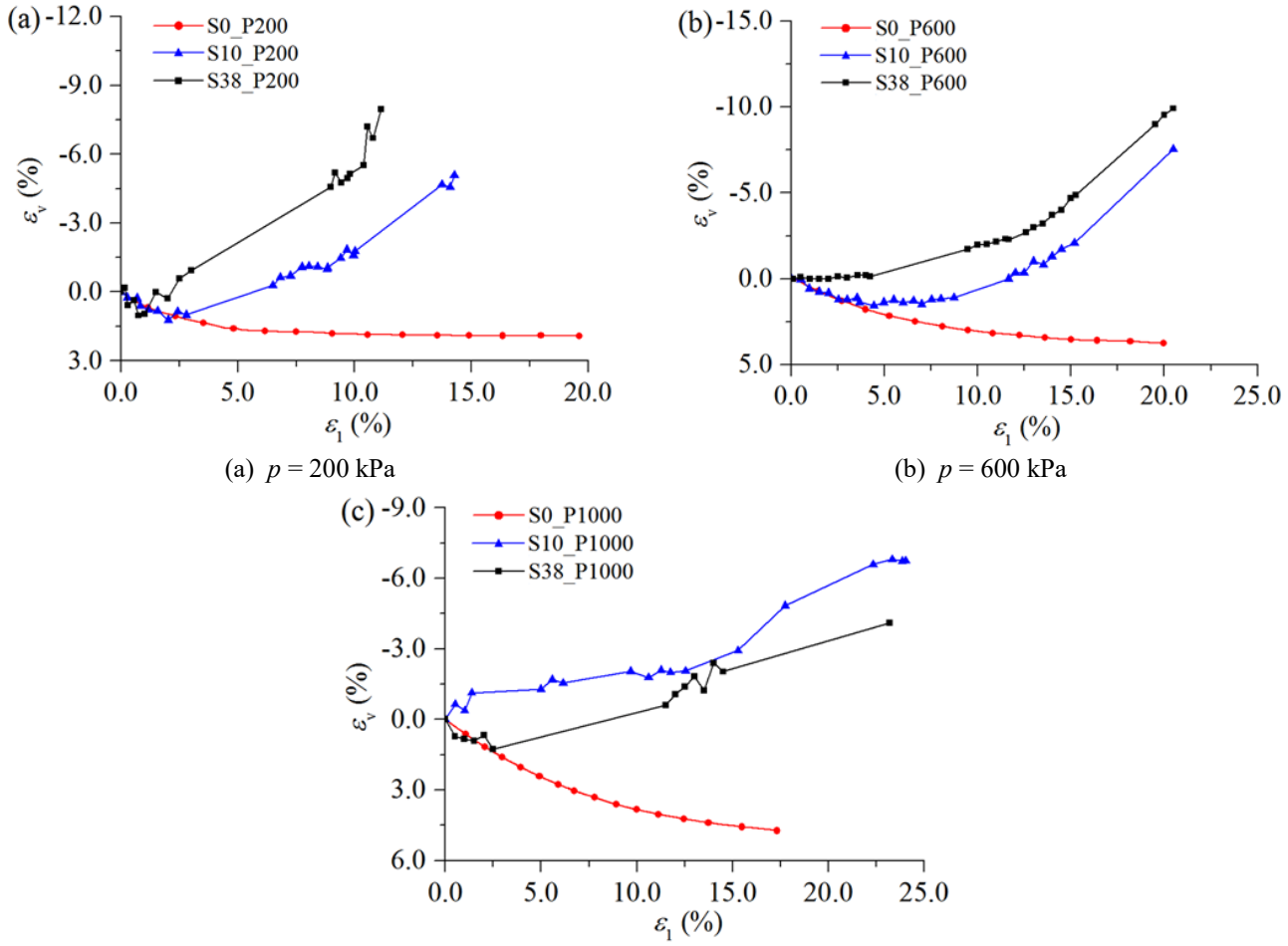

(a) p = 200 kPa (b) p = 600 kPa

(c) p = 1000 kPa

Fig. 20 Volumetric deformation of kaolin clay at the initial suctions of 0 MPa, 10 MPa and 38 MPa

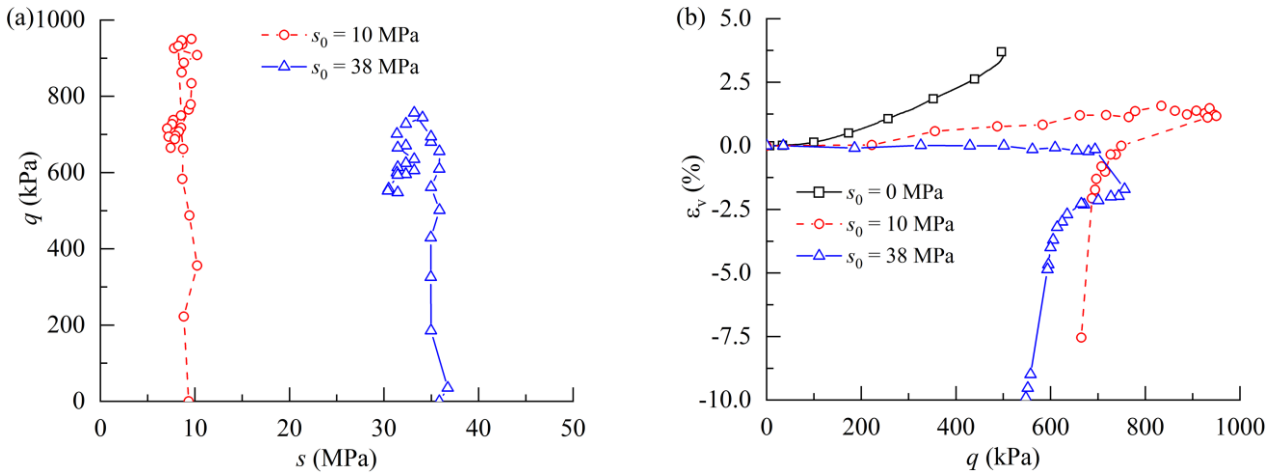

(a) q-s plane (b) q-ε_v plane

Fig. 21 Behavior of unsaturated kaolin clay specimens tested at p = 600 kPa

they cannot measure the volumetric strain of unsaturated soils due to the presence of pore air. Our solution is to incorporate the hygrometer and photographic techniques into the traditional triaxial cell.

The vapor equilibrium method was used to impose and control the initial soil suction during specimen preparation.

Then, two precise hygrometers were used to measure the total suction at the two ends of the specimen during triaxial testing. The volumetric strains were derived from the axial strain measured via the displacement transducer of traditional triaxial cells and the radial strain measured via the photographic technique. The test results show that

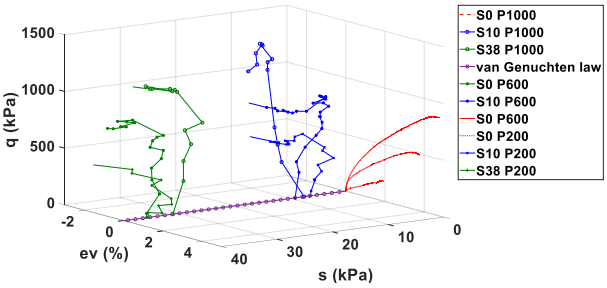

Fig. 22 (s-ε_v-q) plane for all tested soil specimens

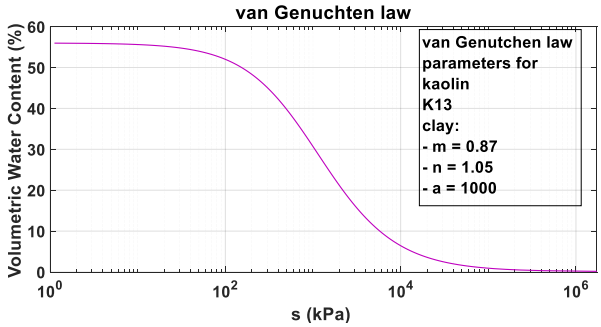

Fig. 23 SWCC of kaolin K13 clay

incorporating the above techniques into a traditional triaxial cell allows for studying the mechanical behavior of unsaturated soils. This improvement is simple and convenient. Most importantly, it does not alter the primary function of the traditional triaxial cell. However, this system also has some limitations related to the precision and range of the used sensors. Moreover, the method used to determine the radial strain and to calculate the volumetric strain need special calibration to obtain precise deformation in unsaturated soil.

Several triaxial test results on specimens with different levels of initial total suction have been presented and discussed. At the beginning of triaxial tests, the measured total suction continuously decreases during both the compression and shearing stages. Also, the peak and residual deviator stresses decrease when the initial total suction increases. In addition, the difference between the maximum deviator stresses at different initial total suctions shows a reducing tendency as the mean stress increases. This result suggests that the effect of suction on the unsaturated shear strength of clay is weakened with increasing mean stress. The total suction has a significant influence on the volumetric behavior of remolded clay under triaxial loading. A marked dilative behavior is observed, which indicates the effect of the capillary cohesion induced by the initial suction.

References

Aversa, S. and Nicotera, M.V. (2002), "A triaxial and oedometer apparatus for testing unsaturated soils", *Geotech. Test. J.*, **25**(1), 3-15. https://doi.org/10.1520/GTJ11075J.

Bella, G. (2021), "Water retention behaviour of tailings in unsaturated conditions", *Geomech. Eng.*, **26**(2), 117-132. https://doi.org/10.12989/gae.2021.26.2.117.

Bhandari, A.R., Powrie, W. and Harkness, R.M. (2012), "A digital image-based deformation measurement system for triaxial tests", *Geotech. Test. J.*, **35**(2), 209-226. https://doi.org/10.1520/GTJ103821.

Biarez, J. (1962), "Contribution à l'étude des propriétés mécaniques des sols et des matériaux pulvérulents", *Thèse de Doctorat*, Grenoble.

Bishop, A.W. and Donald, I.B. (1961), "The experimental study of party saturated soil in the triaxial apparatus", *Proceedings of the 5th Conf. On Soil Mechanics and Found Eng*, Paris, July.

Bishop, A.W. and Green, G.E. (1965), "The influence of end restraint on the compression strength of a cohesionless soil", *Géotechnique*, **15**(3), 243-266.

Blatz, J.A., Cui, Y.J. and Oldecop, L. (2008), "Vapour equilibrium and osmotic technique for suction control", *Geotech. Geol. Eng.*, **26**(6), 661-673. https://doi.org/10.1007/s10706-008-9196-1.

Blatz, J. and Graham, J. (2000), "A system for controlled suction in triaxial tests", *Géotechnique*, **50**(4), 465-469. https://doi.org/10.1680/geot.2000.50.4.465.

Cardoso, R., Sarapajevaite, G., Korsun, O., Cardoso, S. and Ilharco, L. (2017), "Microfabricated sol-gel relative humidity sensors for soil suction measurement during laboratory tests", *Can. Geotech. J.*, **54**(8), 1176-1183. https://doi.org/10.1139/cgj-2016-0419.

Chehade, H.A., Dias, D., Sadek, M., Jenck, O. and Chehade, F.H. (2020), "Upper bound seismic limit analysis of geosynthetic-reinforced unsaturated soil walls", *Geotext. Geomembranes*, **48**(4), 419-430. https://doi.org/10.1016/j.geotexmem.2020.02.001.

Cheng, W.Q., Yang, Z., Hattab, M., Bian, H., Bouchemella, S. and Fleureau, J.M. (2021), "Free desiccation shrinkage process in clayey soils", *Eur. J. Environ. Civil Eng.*, **26**(13), 6398-6423. https://doi.org/10.1080/19648189.2021.1942223.

Delage, P. and Cui, Y. J. (2008), "An evaluation of the osmotic method of controlling suction", *Geomech. Geoeng.*, **3**(1), 1-11. https://doi.org/10.1080/17486020701868379.

Delage, P. (2002), Experimental unsaturated soil mechanics, *Proceedings of the 3rd Int. Conf. on Unsaturated Soils* - UNSAT, Recife, Brazil.

Delage, P., Romero, E. and Tarantino, A. (2008), "Recent developments in the techniques of controlling and measuring suction in unsaturated soils", *In Keynote Lecture, Proceedings of the 1st Eur. Conf. on Unsaturated Soils*, Durham.

Derfouf, F.E.M., Abou-Bekr, N., Taibi, S., Allal, M.A. and Benchouk, A. (2020), "Hydromechanical behaviour of a marl on controlled suction oedometer path", *Eur. J. Environ. Civil Eng.*, **24**(4), 500-519. https://doi.org/10.1080/19648189.2017.1399293.

Estabragh, A.R. and Javadi, A.A. (2012), "Effect of suction on volume change and shear behaviour of an overconsolidated unsaturated silty soil", *Geomech. Eng.*, **4**(1), 55-65. https://doi.org/10.12989/gae.2012.4.1.055.

Fan, S.Y., Song, Z.P., Zhang, Y.W. and Liu, N.F. (2020), "Case study of the effect of rainfall infiltration on a tunnel underlying the roadbed slope with weak inter-layer", *KSCE J. Civil Eng.*, **24**(5), 1607-1619. https://doi.org/10.1007/s12205-020-1165-0.

Ferrari, A., Minardi, A., Ewy, R. and Laloui, L. (2018), "Gas shales testing in controlled partially saturated conditions", *Int. J. Rock Mech. Min. Sci.*, **107**, 110-119, https://doi.org/10.1016/j.ijrmms.2018.05.003.

Fleureau, JM., Kheirbek-Saoud, S., Soemitro, R. and Taibi, S. (1993), "Behaviour of clayey soils on drying-wetting paths", *Can. Geotech. J.*, **30**(2), 287-296, https://doi.org/10.1139/t93-024.

Fleureau, J.M., Hadiwardoyo, S. and Correia, A.G. (2003), "Generalised effective stress analysis of strength and small

strains behaviour of a silty sand, from dry to saturated state", *Soils Found.*, **43**(4), 21-33. https://doi.org/10.3208/sandf.43.4_21.

Fondjo, A.A., Theron, E. and Ray, R.P. (2020), "Assessment of various methods to measure the soil suction", *Int. J. Innov. Tech. Explor. Eng.*, **9**(12), 171-184. https://doi.org/10.35940/ijitee.L7958.1091220.

Fredlund, D.G. and Rahardjo, H. (1993), Soil mechanics for unsaturated soils, John Wiley & Sons.

Gachet, P., Geiser, F., Laloui, L. and Vulliet, L. (2007), "Automated digital image processing for volume change measurement in triaxial cells", *Geotech. Test. J.*, **30**(2), 98-103. https://doi.org/10.1520/GTJ100309.

Gao, Q.F., Hattab, M., Jrad, M., Fleureau, J.M. and Hicher, P.Y. (2020), "Microstructural organization of remoulded clays in relation with dilatancy/contractancy phenomena", *Acta Geotechnica*, **15**(1), 223-243. https://doi.org/10.1007/s11440-019-00876-w.

Garakani, A.A., Sadeghi, H., Saheb, S. and Lamei, A. (2020), "Bearing capacity of shallow foundations on unsaturated soils: analytical approach with 3D numerical simulations and experimental validations", *Int. J. Geomech.*, **20**(3), 04019181, https://doi.org/10.1061/(ASCE)GM.1943-5622.0001589.

Goual, I., Goual, M.S., Taibi, S. and Abou-Bekr, N. (2011), "Behaviour of unsaturated tuff- calcareous sand mixture on drying-wetting and triaxial paths", *Geomech. Eng.*, **3**(4), 267-284. https://doi.org/10.12989/gae.2011.3.4.267.

Hattab, M. and Hicher, P.Y. (2004), "Dilating behaviour of overconsolidated clay", *Soils Found.*, **44**(4), 27-40. https://doi.org/10.3208/sandf.44.4_27.

Hossain, M.A. and Yin, J.H. (2010), "Shear strength and dilative characteristics of an unsaturated compacted completely decomposed granite soil", *Can. Geotech. J.*, **47**(10), 1112-1126. https://doi.org/10.1139/T10-015.

Jiang, T., Zhao, J., Zhang, J., Wang, L., Song, C. and Zhai, T. (2021), "Hydromechanical behavior and prediction of unsaturated loess over a wide suction range", *Geomechanics Eng.*, **26**(3), 275-288. https://doi.org/10.12989/gae.2021.26.3.275.

Kumar, A., Azizi, A. and Toll, D.G. (2022), "Application of suction monitoring for cyclic triaxial testing of compacted soils", *J. Geotech. Geoenviron. Eng.*, **148**(4), 04022009. https://doi.org/10.1061/(ASCE)GT.1943-5606.000276.

Laloui, L., Péron, H., Geiser, F., Rifa'i, A. and Vulliet, L. (2006), "Advances in volume measurement in unsaturated soil triaxial tests", *Soils Found.*, **46**(3), 341-349. https://doi.org/10.3208/sandf.46.341.

Lin, H.D., Wang, C.C. and Wang, X.H. (2018), "A simplified method to estimate the total cohesion of unsaturated soil using an UC test", *Geomech. Eng.*, **16**(6), 599-608. https://doi.org/10.12989/gae.2018.16.6.599.

Mendes, J. and Toll, D.G. (2016), "Influence of initial water content on the mechanical behavior of unsaturated sandy clay soil", *Int. J. Geomechanics*, **16**(6), D4016005, https://doi.org/10.1061/(ASCE)GM.1943-5622.0000594.

Ng, C.W., Zhan, L.T. and Cui, Y.J. (2002), "A new simple system for measuring volume changes in unsaturated soils", *Can. Geotech. J.*, **39**(3), 757-764. https://doi.org/10.1139/t02-015.

Ng, C.W.W., Cui, Y., Rui, C. and Delage, P. (2007), "The axis-translation and osmotic techniques in shear testing of unsaturated soils: a comparison", *Soils Found.*, **47**(4), 675-684. https://doi.org/10.3208/sandf.47.675.

Pan, H., Qing, Y. and Pei-yong, L. (2010), "Direct and indirect measurement of soil suction in the laboratory", *Electron. J. Geotech. Eng.*, **15**(3), 1-14.

Rifa'i, A., Laloui, L. and Vulliet, L. (2002), "Volume measurement in unsaturated triaxial test using liquid variation liquid variation and image processing", *Proceedings of the 3rd Int. Conf. on Unsaturated Soils - UNSAT*, Recife, Brazil.

Shao, L.T., Liu, X., Guo, X.X., Liu, Y. L., Huang, C. and Xue, J. (2020), "Digital image technique for deformation measurement of unsaturated soil specimen in triaxial test", *Unsaturated Soils: Research & Applications*, CRC Press, 1623-1629.

Sivakumar, V., Kodikara, J., O'hagan, R., Hughes, D., Cairns, P., and McKinley, J.D. (2013), "Effects of confining pressure and water content on performance of unsaturated compacted clay under repeated loading", *Géotechnique,* **63**(8), 628-640. https://doi.org/10.1680/geot.10.P.103.

Sreedeep, S. and Singh, D.N. (2011), "Critical review of the methodologies employed for soil suction measurement", *Int. J. Geomech.*, **11**(2), 99-104. https://doi.org/10.1061/(ASCE)GM.1943-5622.0000022.

Wei, X., Hattab, M., Taibi, S., Bicalho, K.V., Xu, L., and Fleureau, J.M. (2021), "Crack development and coalescence process in drying clayey loess", *Geomech. Eng.*, **25**(6), 535-552. https://doi.org/10.12989/gae.2021.25.6.535.

Zhao, D., Gao, Q.F., Hattab, M., Hicher, P.Y. and Yin, Z.Y. (2020), "Microstructural evolution of remolded clay related to creep", *Transport. Geotech.*, **24**, 100367, https://doi.org/10.1016/j.trgeo.2020.100367.

Zhao, D., Hattab, M., Yin, Z.Y. and Hicher, P.Y. (2019), "Dilative behavior of kaolinite under drained creep condition", *Acta Geotechnica*, **14**(4), 1003-1019. https://doi.org/10.1007/s11440-018-0686-x.

Zhou, N.Q., Zhao, S., Song, W. and Otani, J. (2014), "Contaminant migration in unsaturated porous media using X-ray computerized tomography (CT)", *Water Sci. Technol.,* **69**(5), 953-959. https://doi.org/10.2166/wst.2013.801.

CC